



UNIVERSITY  
OF WOLLONGONG  
AUSTRALIA

University of Wollongong  
Research Online

---

Faculty of Engineering and Information Sciences -  
Papers: Part A

Faculty of Engineering and Information Sciences

---

2014

# Effect of ballast contamination on the behaviour of track substructure

Nayoma Tennakoon

*University of Wollongong, [nayoma@uow.edu.au](mailto:nayoma@uow.edu.au)*

Buddhima Indraratna

*University of Wollongong, [indra@uow.edu.au](mailto:indra@uow.edu.au)*

Cholachat Rujikiatkamjorn

*University of Wollongong, [cholacha@uow.edu.au](mailto:cholacha@uow.edu.au)*

---

## Publication Details

Tennakoon, N., Indraratna, B. & Rujikiatkamjorn, C. (2014). Effect of ballast contamination on the behaviour of track substructure. *Australian Geomechanics Journal*, 49 (4), 113-123.

Research Online is the open access institutional repository for the University of Wollongong. For further information contact the UOW Library:  
[research-pubs@uow.edu.au](mailto:research-pubs@uow.edu.au)

---

# Effect of ballast contamination on the behaviour of track substructure

## **Abstract**

Ballast contamination by subgrade pumping and coal contamination is understood as major cause of track deterioration in many countries over the world. As contamination clogs the ballast voids, the drainage capacity of the track is compromised. Further, lubrication caused by these fines results in reducing load bearing capacity of the ballast layer. In this study, a series of large scale hydraulic conductivity and triaxial tests were performed to study the influence of contamination of ballast on its drainage and shear strength characteristics. Drainage capacity of the contaminated track under different level of contamination was determined, undertaking a numerical analysis using Seep/W. Shear strength of coal and clay contaminated ballast at different confining pressures were compared. Bearing capacity of contaminated track, using 'foundation under three layers' method was derived and plotted against the degree of contamination. Subsequently, the critical level of contamination by fouling materials such as clay and coal is discussed on the basis of hydraulic conductivity, shear strength and bearing capacity of the ballast.

## **Disciplines**

Engineering | Science and Technology Studies

## **Publication Details**

Tennakoon, N., Indraratna, B. & Rujikiatkamjorn, C. (2014). Effect of ballast contamination on the behaviour of track substructure. *Australian Geomechanics Journal*, 49 (4), 113-123.

# EFFECT OF BALLAST CONTAMINATION ON THE BEHAVIOUR OF TRACK SUBSTRUCTURE

N. Tennakoon<sup>1</sup>, B. Indraratna<sup>2</sup> and Cholachat Rujikiatkamjorn<sup>3</sup>

<sup>1</sup> Research Fellow, <sup>2</sup> Professor, <sup>3</sup> Associate Professor, Centre for Geomechanics and Railway Engineering, Faculty of Engineering and Information Sciences, University of Wollongong, Wollongong City, Australia

## ABSTRACT

Ballast contamination by subgrade pumping and coal contamination is understood as major cause of track deterioration in many countries over the world. As contamination clog the ballast voids, the drainage capacity of the track is compromised. Further, lubrication caused by these fines results in reducing load bearing capacity of the ballast layer. In this study, a series of large scale hydraulic conductivity and triaxial tests were performed to study the influence of contamination of ballast on the conditions of its drainage and shear strength. Drainage capacity of the contaminated track was determined, undertaking a numerical analysis using Seep/W under different level of contamination. Shear strength of coal and clay contaminated ballast at different confining pressures were compared. Bearing capacities of contaminated track, using foundation under 3 overlying layers method were derived and plotted against the degree of contamination. Subsequently, the critical level of contamination by fouling materials such as clay and coal is discussed on the basis of hydraulic conductivity, shear strength and bearing capacity of the ballast.

## 1 INTRODUCTION

Railway ballast consists of coarse angular aggregates between 10-60 mm in size placed underneath the sleeper. Figure 1 shows a typical cross section of a ballasted track. For track serviceability, safety and longevity, it is crucial to maintain the ballast layer to be relatively clean. However, during track operation, fine particles can accumulate within the ballast voids due to: (a) breakage of angular rock particles, (b) infiltration of fines from the surface including coal, and (c) pumping of unstable subgrade soil under excessive cyclic loads (Indraratna et al., 2011a and Selig and Waters, 1994). This contamination (fouling) can decrease overall shear strength and impede drainage of the track.

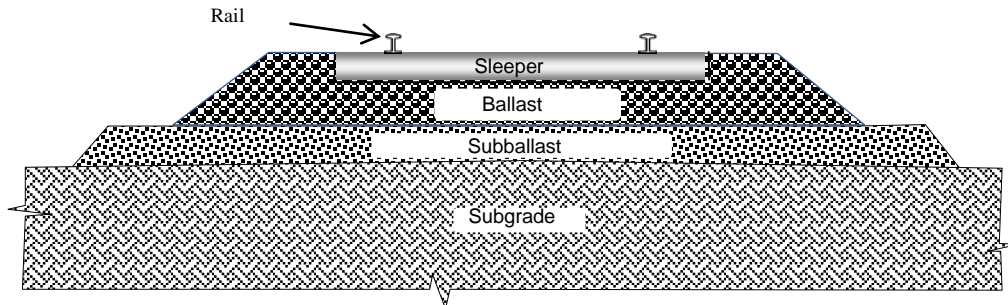


Figure 1: Typical ballasted railway track cross section.

In low-lying coastal areas where the subgrade is usually saturated, the finer silt and clay particles may pump in a liquefied form into the ballast layer during the passage of a fast moving train, especially in the absence of a proper filtration layer or geosynthetics underneath the ballast layer (Indraratna et al, 2002 and Selig and Waters, 1994). During transport, coal particles falling off the overfilled wagons usually cause significant ballast contamination over time. In Australia, clay (subgrade) and coal contamination can be commonly encountered (Figure 2). This paper addresses the effects of coal and clay contamination on track drainage and shear strength with the associated implications on the bearing capacity.



Figure 2: Ballast contamination due to (a) clay pumping in Ashfield, New South Wales, Australia and, (b) coal contamination in Rockhampton, Queensland, Australia

## 2 TRACK DRAINAGE

Drainage plays an important role in the stability of railroad substructure. When the ballast layer is contaminated, fine particles clogging its voids may significantly decrease the track drainage capacity causing the build-up of excess pore water pressure under imposed train loading, often making the track inoperative and unstable. A series of constant head hydraulic conductivity tests (Tennakoon et al, 2012) were conducted using a large-scale permeameter (Figure 3), in which different levels of contamination were examined to establish a relationship between the void contamination index and the hydraulic conductivity. This apparatus can accommodate specimens up to 500 mm in diameter and 1000 mm in height. A filter membrane was placed below the layer of ballast while maintaining a free drainage boundary. The test specimen was placed above the filter membrane and compacted in four equal layers to represent a typical field unit weight of  $16.0\text{--}16.5\text{ kN/m}^3$ . Commercial kaolin and pulverised coal were used to simulate the track contaminants. The gradations of fines together with the ballast used for laboratory testing are plotted in Figure 4. Detailed test procedure has been explained elsewhere by Tennakoon et al, (2012).

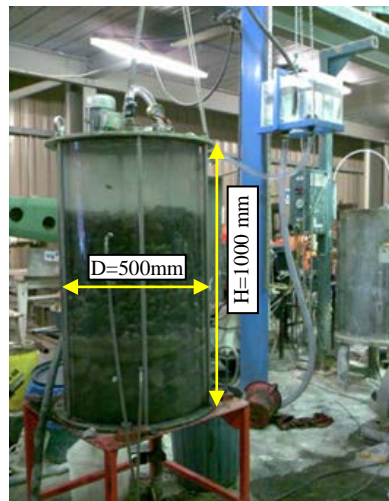


Figure 3: Large scale permeability test apparatus

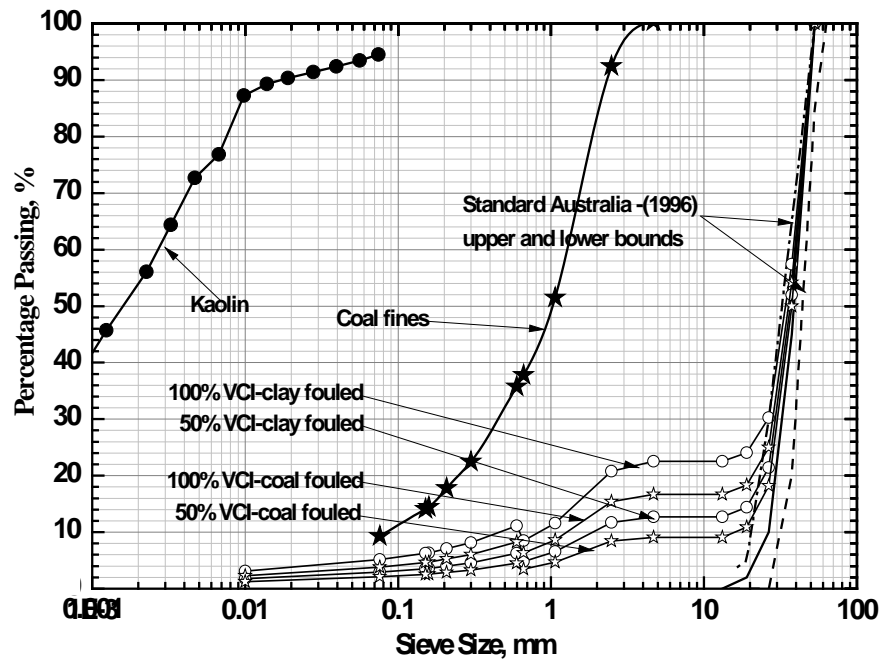


Figure 4: Gradations of clean ballast and contaminated materials

Volume based contamination indices can accurately capture the extent of contamination (Tennakoon et al, 2012, Indraratna et al, 2013, Feldmen and Nissen, 2002), when different fouling materials have different specific gravities. The Void Contaminant Index (*VCI*) defined as the ratio of the bulk volume of contamination to the volume of voids in clean ballast is used to quantify degree of ballast contamination.

Table 1 shows the experimental results for coal and clay contaminated ballast with different degrees of contamination. As expected, the hydraulic conductivity decreases when the degree of contamination increases. However, coal contaminated ballast shows a lesser reduction in hydraulic conductivity compared to the clay-fouled ballast at a higher degree of contamination (*VCI* >50%). Moreover, at a lower degree of contamination (*VCI* <50%), clay-fouled ballast yields a higher hydraulic conductivity than the coal-fouled ballast. This is because, at low levels of contamination, cohesive clay particles simply attach to the surface of the ballast aggregates (less void filling), while cohesionless coal material accumulates and compacts at the bottom of the specimen impeding drainage. For a larger degree of contamination, the overall hydraulic conductivity of ballast is mainly governed by the hydraulic conductivity of the contaminated material itself. More details about hydraulic conductivity of fouled ballast can be found in Tennakoon et al, 2012.

Table 1: Experimental results of hydraulic conductivity for clay-fouled and coal-fouled ballast

<i>VCI</i> , %	Hydraulic Conductivity, m/s	
	Clay contaminated ballast	Coal contaminated ballast
0	$3.61 \times 10^{-01}$	$3.61 \times 10^{-01}$
25	$2.08 \times 10^{-02}$	$3.78 \times 10^{-04}$
50	$1.35 \times 10^{-04}$	$1.50 \times 10^{-04}$
75	$8.19 \times 10^{-07}$	$1.10 \times 10^{-04}$
100	$2.45 \times 10^{-08}$	$9.74 \times 10^{-05}$

To predict track drainage, a finite element analysis employing the software SEEP/W (GeoStudio 2007 a/b) was conducted to simulate two-dimensional flow within a typical track substructure. Laboratory evaluated values of hydraulic conductivity (Table 1) were used as input parameters. Exploiting track symmetry, it was sufficient to model one half of the track as shown in Figure 5. When modeling the clay contaminated ballast, the clay material was considered to be uniformly distributed. While non-uniform distribution was considered for coal contaminated ballast since coal can be settled down at the bottom of the ballast layer.

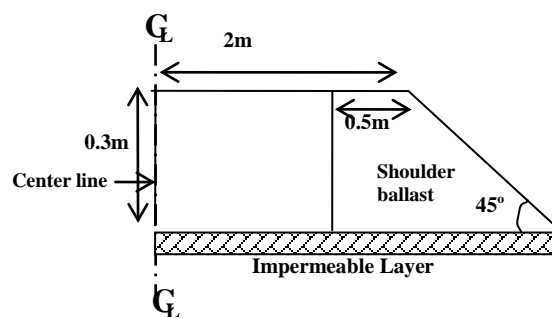


Figure 5: Vertical cross section of the typical ballast layer used in seepage analysis

The drainage classification as described earlier by Tennakoon et al, (2012) was adopted in this study. The maximum rainfall intensity of 150 mm/h (Pilgrim, 1997) which corresponds to a flow rate (critical flow rate,  $Q_c$ ) of  $0.0002 \text{ m}^3/\text{s}$  over the unit length of the track was considered in this FEM analysis. The drainage capacity ( $Q$ ) of the contaminated ballast could be obtained for different degrees of contamination. When  $Q$  is equal to or lower than  $Q_c$  (i.e. track becomes saturated under a given rainfall), then the track condition can be classified as 'poor drainage'. The ratio of  $Q/Q_c$  as reported by Tennakoon et al, 2012 was used to classify the overall track drainage conditions.

Figure 6 presents the results obtained from the SEEP/W analysis, which shows that when the entire track is contaminated by clay  $> 35\%$   $VCI$ , the drainage condition of the track is not acceptable. However, for coal contaminated ballast, track can continue to perform well until a  $VCI$  approaches about 65%. A dramatic reduction in  $Q/Q_c$  can be observed for  $VCI > 75\%$  for clay contaminated ballast, while for coal contaminated ballast this reduction becomes marginal. This is because the permeability of contaminated ballast approaches that of the fouling material (contaminant) itself. It is noted that the coal-contaminated ballast reached this critical value faster than the clay-contaminated ballast. These results are used later in conjunction with the shear behaviour of clay-contaminated ballast to estimate the critical level of contamination.

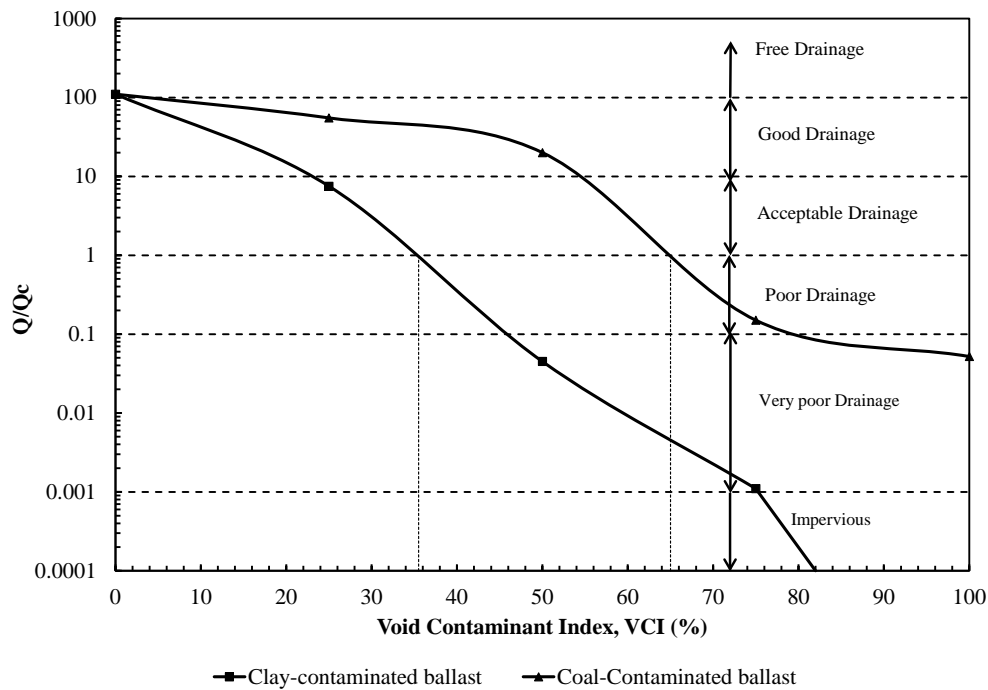


Figure 6: Variation of  $Q/Q_c$  ratio with degree of contamination ( $VCI$ )

### 3 SHEAR STRENGTH OF CONTAMINATED BALLAST

A series of large-scale monotonic and cyclic triaxial tests were carried out to understand the effect of clay contamination on the stress-strain and degradation behaviour of ballast. Different contamination levels ( $VCI = 0\%$  to  $80\%$ ) and a confining pressure ( $\sigma'_3$ ) of  $10\text{ kPa}$  were adopted to simulate typical field conditions. A  $7\text{ mm}$  thick cylindrical rubber membrane was used to prepare and confine the ballast specimen. The  $PSD$  of clean ballast was used as per the recommended Australian Standards (Figure 4), where the maximum grain size falls between  $50$  and  $60\text{ mm}$ . Commercial kaolin was used to mimic the fine clay contaminant. The amount of clay needed for a given value of  $VCI$  was determined for each test specimen. Further details of specimen preparation have been elaborated elsewhere by Indraratna et al., 2013.

Indraratna et al., 2011b performed a series of direct shear testing on coal-contaminated ballast. These results were compared with clay-contaminated ballast, as described below.

#### 3.1 Shear strengths of contaminated ballast

For a granular rockfill, the following non-linear shear strength envelope reported by Indraratna et al., 2013 and Indraratna et al., 2011b could be applied for both fresh and contaminated ballast:

$$\frac{\tau_f}{\sigma_c} = m \left( \frac{\sigma'_n}{\sigma_c} \right)^n \tag{ 1 }$$

where,  $\tau$ ,  $\sigma'_n$  and  $\sigma_c$  are shear stress, effective normal stress and uniaxial compressive strength of the parent rock ( $130\text{ MPa}$ ). Shear stresses were determined based on the peak stress value from the stress-strain curves. The values of  $m$  and  $n$  in Eqn. (1) are empirical coefficients which vary with  $VCI$ , and they can be established by best-fit (regression) analysis ( $r^2 > 0.95$ ) by the following expressions for clay-fouled ballast:

$$m = 0.07[1 + \tanh(VCI/21.5)] \tag{ 2 }$$

$$n = 0.56[1 + 0.3\tanh(VCI/21.5)] \tag{ 3 }$$

Table 2 shows the m and n parameters for coal-contaminated ballast for fresh and three levels of VCI.

Table 2: m and n parameters for coal contaminated ballast

VCI	m	n
0	0.24	0.75
20	0.23	0.76
40	0.23	0.77
70	0.25	0.8

Consequently, the strength reduction factor as proposed in Equation 4 was determined and plotted in Figure 7 in comparison with the clay-contaminated ballast.

$$\text{Strength Reduction Percentage} = \left( \frac{q_{peak,b} - q_{peak,f}}{q_{peak,b}} \right) \times 100 \tag{ 4 }$$

Figure 7 shows the strength reduction percentage for clay and coal-contaminated ballast with varying confining pressure. It is clear that the reduction in strength is greater for clay-fouled ballast at all levels of contamination, as the lubrication effect is more prevalent for plastic fines compared to the non-plastic (granular) fines such as coal. Interestingly, the strength reduction seems to be decreasing with increasing of confining pressure. Therefore, at low confining pressure that is typical of field track conditions, the strength reduction is usually considerable.

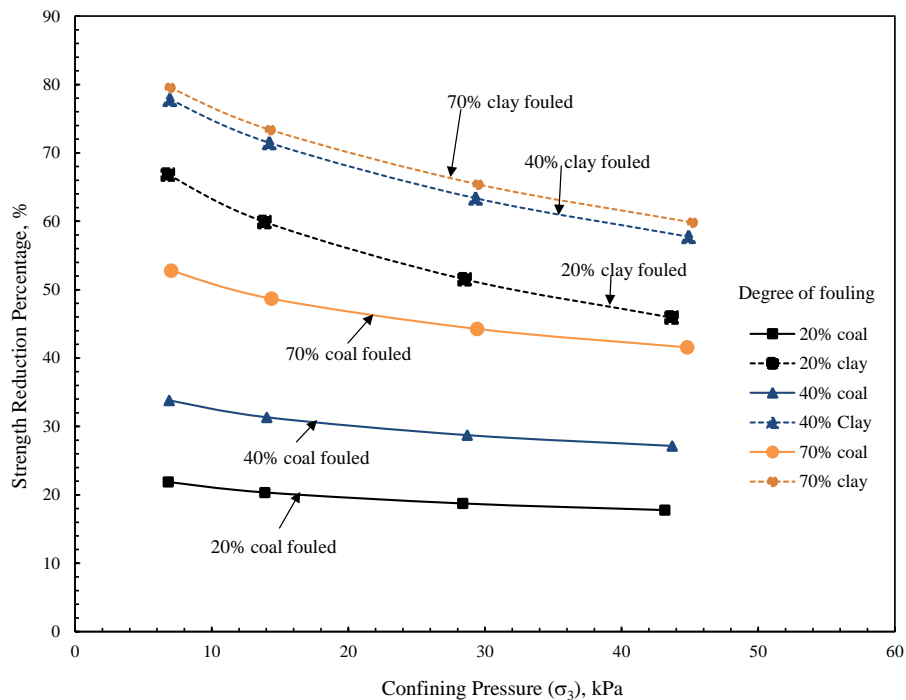


Figure 7: Comparison of shear strength reduction of clay-contaminated and coal-contaminated ballast



### 3.2 RESILIENT BEHAVIOR OF CLAY CONTAMINATED BALLAST

In order to investigate the resilient behavior of clay-contaminated ballast, a series of cyclic loading testing were performed. The cyclic load was varied between the maximum deviatoric stress ( $q_{max}$ ) of 230kPa and the minimum deviatoric stress ( $q_{min}$ ) of 45 kPa which represents the state of cyclic loading during the passage of a 25 tonne axle train as recorded by field monitoring (Indraratna et al. 2010a/b; Indraratna et al. 2011a).

For a relative cyclic stress ( $n$ ) defined by Suiker (2005) as shown in Equation 5, tabulates the value of  $n$  for varying levels of VCI. These 'n' values were calculated using the maximum  $q/p$  ratios derived from the monotonic loading results obtained for clay-contaminated ballast by Indraratna et al, 2012. As shown in Figure 8, the value of  $n$  increases with an increase in VCI resulting in greater axial strains.

$$n = \frac{(q/p)_{cyc}}{(q/p)_{stat,max}} \quad ( 5 )$$

where,  $q$  is the deviator stress and  $p$  is the mean stress.

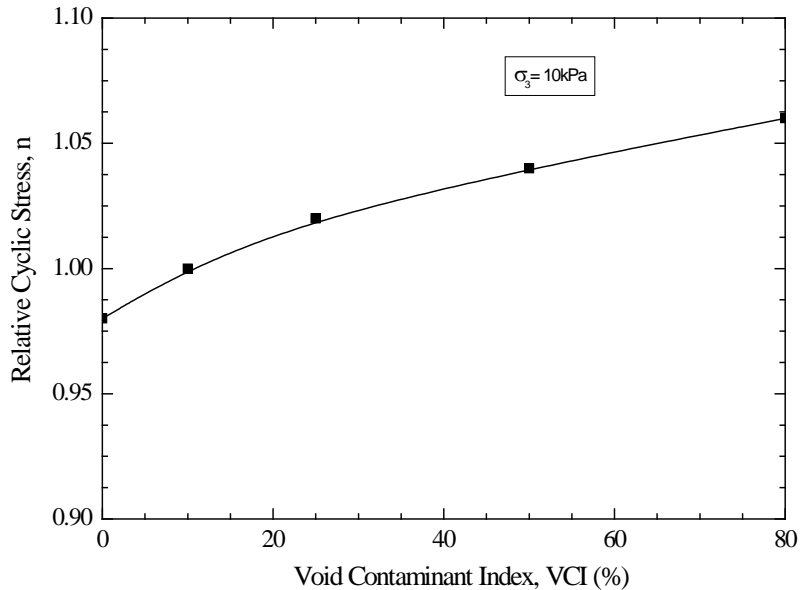


Figure 8: Variation of relative cyclic stress ( $n$ ) with VCI

Resilient modulus,  $M_r$  was calculated using Equation 6, where  $\Delta_{q,cyc}$  is the magnitude of deviator stress (Eqn. 7), and  $\epsilon_{a,rec}$  is the recoverable portion of axial strain.

$$M_r = \frac{\Delta_{q,cyc}}{\epsilon_{a,rec}} \quad ( 6 )$$

$$\Delta_{q,cyc} = q_{max} - q_{min} \quad ( 7 )$$

Figure 9 shows the variation of the resilient modulus at  $N=1000$  and  $N=500,000$  cycles with VCI together with the drainage zones obtained from Figure 6. At increased number of cycles, the resilient modulus shows a significant improvement due to cyclic densification as reported by Tennakoon and Indraratna, 2014. An increased level of

contamination indicates a decrease in  $M_r$ . In Australia, especially during wet periods where the risk of mud pumping is high, implementation of speed restrictions is common. It can also be seen that at higher number of loading cycles, there is a significant reduction in  $M_r$ , whereas at a small number of cycles, the reduction in  $M_r$  is only marginal. It should be noted that at 500,000 cycles where poor drainage is inevitable at 35% VCI, the reduction in  $M_r$  is more than 20%.

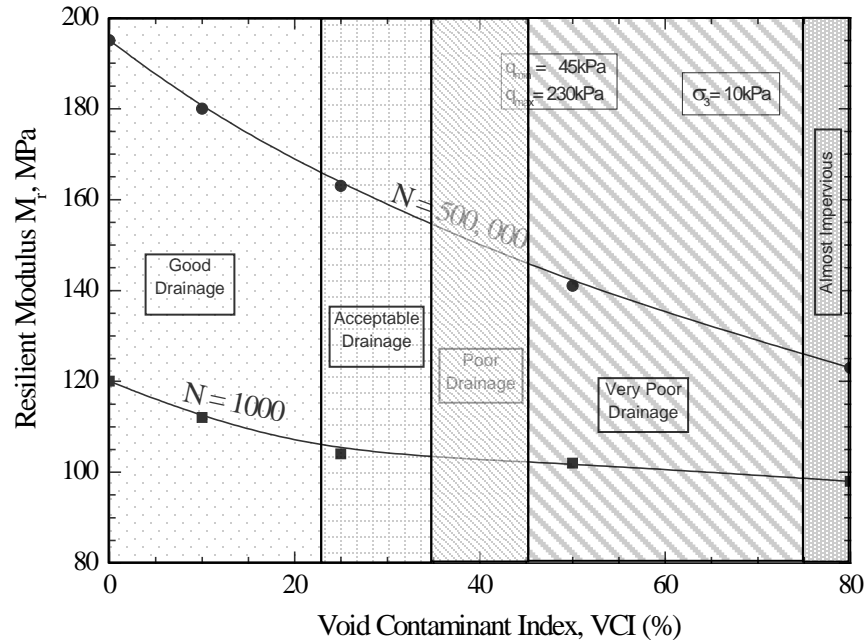


Figure 9: Variation of resilient modulus at  $N=1000$  and  $N=500,000$  cycles vs. void contaminant index.

#### 4 EFFECT OF CONTAMINATION ON BEARING CAPACITY OF TRACK SUBSTRUCTURE

There have been numerous attempts made in the past for determining the bearing capacity of a layered soil (e.g. Hansen, 1970; Meyerhof, 1974; Meyerhof & Hanna, 1978; Hanna & Meyerhof, 1980; Bowles, 1988; Chen and Davidson 1973; Reddy and Srinivasan 1967, and Broms, 1965). Among the above methods, Hanna and Meyerhof (1980) approach works well for granular material overlying a weak subgrade (Sattler et al., 1989). Therefore, this method proposed by Hanna and Meyerhof (1979) for a foundation consisting of 3 layers (weakest layer at the bottom) was adopted in this study to analyse a rail track (Figure 10). Here, the failure mechanism assumes that a soil mass of the upper granular layer (approximately pyramidal shape) is pushed into the lower subgrade (i.e. soft soil layer). At limit equilibrium, the sum of forces in the vertical direction contributes to the ultimate bearing capacity ( $q_u$ ).

It should be noted that the non-symmetric geometry may affect the shape of failure mechanism. However, any effects due to crib and shoulder ballast on the shape of failure mechanism are neglected in the current study. In rail track environment, maximum stress concentration occurs below rail (Indraratna et al. 2010). Considering this, the failure mechanism is assumed as symmetrical about the vertical line passing through the wheel-rail contact point.

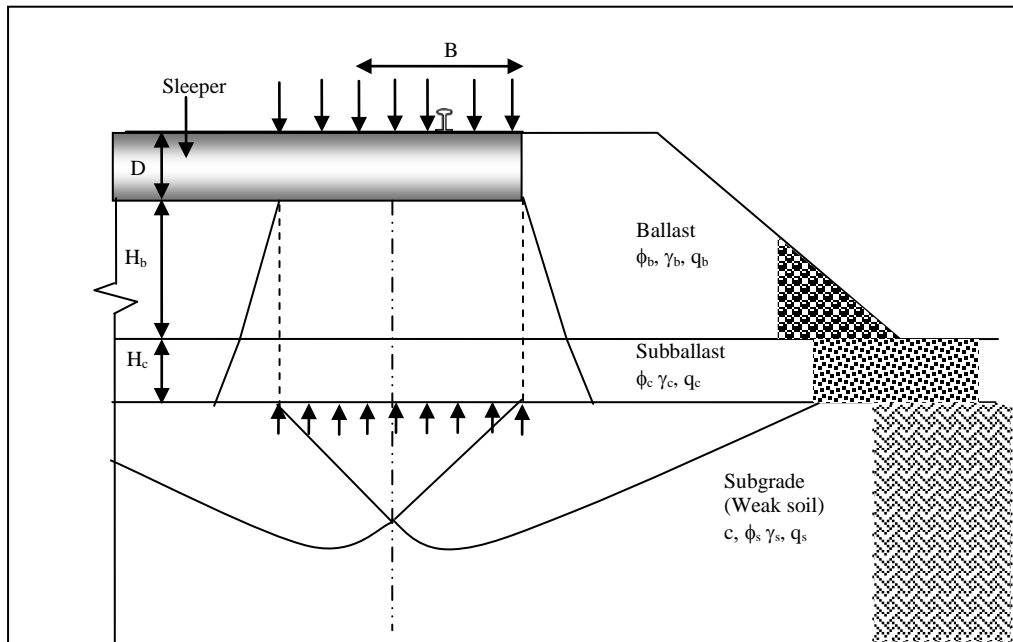


Figure 10 : Failure of track substructure below sleeper on ballast, subballast(capping) layers overlying weak subgrade

(Modified after Hanna and Meyerhof, 1979)

The Authors have modified and rewritten the ultimate bearing capacity equation initially proposed by Hanna and Meyerhof (1979) for a ballasted track as (Figure 10):

$$q_u = q_s + K_{sb} \frac{\bar{\gamma} H_b^2 \tan \phi_b}{B} \left( 1 + \frac{2D}{H_b} \right) + K_{sc} \frac{\bar{\gamma} H_c^2 \tan \phi_c}{B} \left( 1 + \frac{2(H_b + D)}{H_c} \right) - \bar{\gamma}(H_b + H_c) \leq q_b \quad (8)$$

where;

$q_u$  = Ultimate bearing capacity of rail substructure (Containing 3 layers)

$q_s$  = Ultimate bearing capacity on a very thick bed of weak subgrade

$q_b$  = Ultimate bearing capacity of very thick layer of ballast

$\bar{\gamma}$  = Average unit weight of the upper layers (i.e ballast and subballast)

$K_{sb}$  = Punching shear coefficient for the ballast layer (Determined from published charts, Meyerhof & Hanna, 1978)

$K_{sc}$  = Punching shear coefficient for the subballast (capping) layer (Determined from published charts, Meyerhof & Hanna, 1978)

D = depth of the crib ballast

$H_b$  = depth of the ballast layer underneath the sleeper

$H_c$ = depth of the subballast (capping) layer

$B$ = Effective length of the sleeper (1/3 of the length of a sleeper)

$K_{sb}$  was calculated based on the ratio of  $q_c/q_b$  and friction angle of  $\phi_b$ .  $K_{sc}$  was calculated based on the ratio of  $q_s/q_c$  and friction angle of  $\phi_c$ . where  $q_b$ ,  $q_c$  and  $q_s$  are the ultimate bearing capacities of strip footing under vertical load on the surface of homogeneous thick beds of ballast, subballast and subgrade respectively (Meyerhof and Hanna, 1978)

In this study, track data monitored by the Authors in the town of Singleton (NSW) was used to determine the ultimate bearing capacity of the track substructure as detailed in Table 3. The friction angles of contaminated ballast were obtained experimentally as reported by reported by Indraratna et al., 2013 and Indraratna et al., 2011b. The ultimate bearing capacity (Eqn. 8) for clay and coal fouled ballast as a function of  $VCI$  is plotted in Figure 11.

Table 3: Input parameters to calculate the bearing capacity

$H_b$ , m	0.3	
$H_c$ , m	0.9	
$\phi_b$ , °	Clay contaminated	Coal Contaminated
	57 (0% $VCI$ )	57 (0% $VCI$ )
	52 (10% $VCI$ )	54 (10% $VCI$ )
	49 (25% $VCI$ )	53 (25% $VCI$ )
	46 (50% $VCI$ )	49 (50% $VCI$ )
45 (80% $VCI$ )	47 (80% $VCI$ )	
$\phi_c$ , °	45	
$\phi_s$ , °	20	
$D$ , m	0.15	
$B$ , m	0.8	
$\gamma_b$ , kN/m <sup>3</sup>	15.7	
$\gamma_c$ , kN/m <sup>3</sup>	18	
$c$ , kPa	10	

Figure 11 shows that the bearing capacity decreases with an increased level of clay and coal contamination. Coal-contaminated ballast shows a higher bearing capacity compared to that of clay-contaminated ballast, and this is because the coal-contaminated ballast has a higher friction angle. In order to understand the effect of ballast depth and undrained shear strength of subgrade on the bearing capacity, the ballast depth and undrained shear strength were varied in Equation 8 and the corresponding results plotted in Figure 12 (a,b). It can be seen that an increase in ballast depth leads to an increase in the overall bearing capacity. Increase in undrained shear strength of subgrades, increased the ultimate bearing capacity linearly. The value of the undrained strength can be determined from the laboratory data or performing Vane shear test in field.

For example, a 20t load train (wheel diameter= 0.97m) passing at 60km/h over a concrete sleeper of 0.225m width and 2.7 m length will generate a pressure of about 320kPa on top of the ballast layer. However, Figure 11 shows that the bearing capacity is not sufficient to accommodate this train load, and therefore it is recommended to increase the thickness of the granular layer according to the subgrade conditions and the level of contamination of ballast.

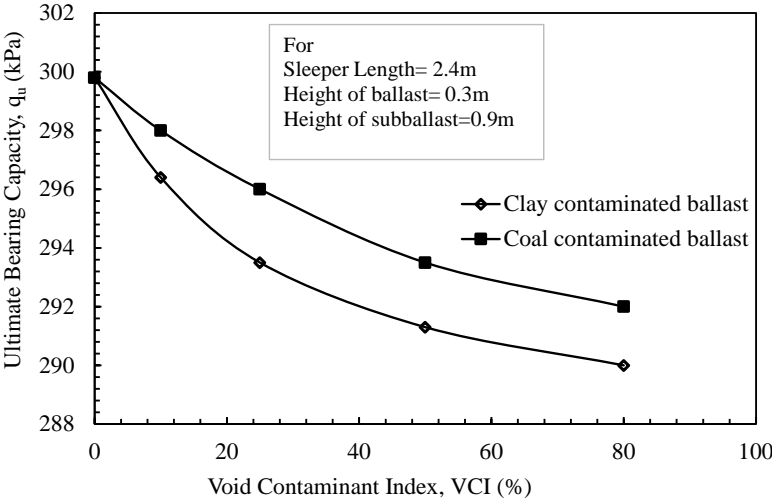
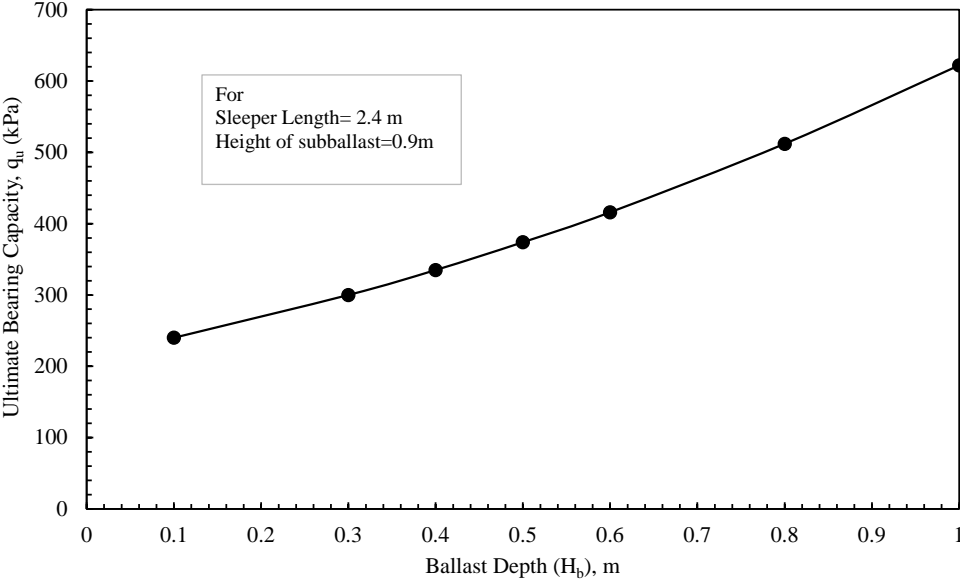
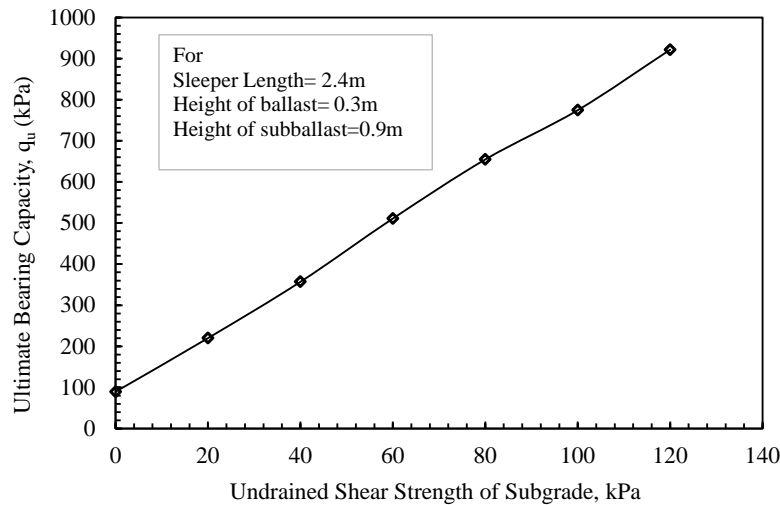


Figure 11 : Variation of bearing capacity of clay-contaminated ballast with VCI



(a)



(b)

Figure 12 : Effect of (a) ballast depth and (b) undrained shear strength of subgrade, on bearing capacity of the track substructure for fresh ballast ( $VCI=0\%$ )

## 5 CONCLUSIONS

Rail ballast becomes contaminated by the infiltration of fines such as subgrade clay and silt, as well as coal particles along the freight corridors. In this paper, detrimental effects of contamination on drainage, strength and bearing capacity aspects of ballasted tracks under various levels of contaminations were discussed using the Void Contaminant Index ( $VCI$ ). A relationship between  $VCI$  and the hydraulic conductivity of fouled ballast was established using a large-scale permeameter. It was found that coal-contaminated ballast shows a lesser reduction in hydraulic conductivity compared to clay-fouled ballast when  $VCI > 50\%$ . Moreover, when  $VCI < 50\%$ , clay-fouled ballast shows a higher hydraulic conductivity than coal-fouled ballast. This is because, at low contamination levels, clay particles simply attach to the ballast surface, while coal particles tend to accumulate and compact at the bottom of the specimen, thereby impeding drainage. Based on numerical analysis, when the entire track is contaminated by clay  $> 35\%$   $VCI$ , the drainage condition of the track is not acceptable. However, for coal-contaminated ballast, track can continue to perform reasonably well until  $VCI$  approaches about 65% before maintenance becomes crucial.

A series of large-scale monotonic and cyclic triaxial tests were carried out to understand the effect of clay fouling (contamination) on the stress-strain and degradation behaviour of ballast. It is clear from the current test results that the reduction in strength is greater for clay-fouled ballast, as the 'lubrication' effect attributed to clay coating of the aggregate surface is more prevalent for plastic fines compared to the non-plastic (granular) fines such as coal. This strength reduction becomes less prominent when the confining pressure increases. At low confining pressure that is typical of field conditions, the strength reduction is usually marked, and this clearly reflects the negative implications of subgrade clay fouling of ballast. At increased number of cycles, the resilient modulus of ballast shows a significant increase due to cyclic densification of particles. When  $VCI$  is more than 35%, the reduction in the resilient modulus exceeds 20% at 500,000 cycles.

Based on the track data monitored by the Authors in the town of Singleton (NSW), a layered track structure was analysed to obtain its ultimate bearing capacity. The overall bearing capacity decreases with an increased level of clay and/or coal contamination. Not surprisingly, coal-fouled ballast showed a higher bearing capacity compared to that of clay-fouled ballast, and this is because the former was characterised by a higher angle of friction. It can also be seen that an increase in ballast depth leads to an increase in the overall bearing capacity.

## 6 ACKNOWLEDGEMENTS

The Authors wish to thank the CRC for Railway Innovation and Australian Research Council (ARC) for their funding of this research and those geotechnical organisations who have given support over the years. In particular, sincere thanks to Sydney Trains (previously, RailCorp), ARTC and Aurizon (previously, QR National). The assistance provided by senior technical officers, Mr. Alan Grant, Mr. Ian Bridge, and Mr. Cameron Neilson is also appreciated. More elaborate details of the contents discussed in the paper can be found in previous publications by the Authors in the *Géotechnique* and *ASTM Geotechnical Testing Journal*, as cited in the text and listed below.

## 7 REFERENCES

- Bowles, J. E. *Foundation analysis and design*. McGraw-Hill Book Company, New York. 1988.
- Broms, B. B. Effect of degree of saturation on bearing capacity of flexible pavements, 43<sup>rd</sup> Annual meeting of the committee on Flexible pavement design, Ithaca, New York. 1965.
- Chen, W. F. and Davidson, H. L. Bearing Capacity Determination by Limit Analysis. *J. Soil Mech. Found. Div., ASCE*, 1973,99(6): p. 433-449.
- Feldman, F. and Nissen, D. Alternative testing method for the measurement of ballast fouling, Conference on Railway Engineering RTSA, Wollongong NSW, Australia, 2002: p.101-109.
- GeoStudio. *GeoStudio Tutorials includes student edition lessons*, 1st edn. Geo-Slope International Ltd., Calgary. 2007a
- GeoStudio, *Seep/W for finite element seepage analysis, users manual*. Geo-Slope International Ltd., Calgary, Alberta, Canada. 2007b.
- Hanna A.M. & Meyerhof G.G. Ultimate bearing capacity of foundations on a three-layer soil, with special reference to layered sand," *Canadian Geotechnical Journal*. 1979.16(2): p.412-414.
- Hanna, A. M., and Meyerhof, G.G . Design Chart for ultimate bearing capacity of foundations on sand overlying soft clay. *Canadian Geotech. J.*, 1980.17(2): p.300-303
- Hansen, J. B. A revised and extended formula for bearing capacity. *Geotekniks Inst., Bull.*, 1970. 28:p.5-11.
- Indraratna B, Nimbalkar S, Christie D, Rujikiatkamjorn C and Vinod JS Field assessment of the performance of a ballasted rail track with and without geosynthetics. *Journal of Geotechnical and Geoenvironmental Engineering ASCE*. 2010a. 136(7) : p.907-917.
- Indraratna B, Rujikiatkamjorn C, Adams M and Ewers B Class A prediction of the behaviour of soft estuarine soil foundation stabilised by short vertical drains beneath a rail track. *International Journal of Geotechnical and Geoenvironmental Engineering, ASCE*. 2010b. 136(5): p.686-696.
- Indraratna B, Salim W and Rujikiatkamjorn C. *Advanced Rail Geotechnology – Ballasted Track*. CRC Press,Balkema, 2011a: 414p.
- Indraratna, B., Khabbaz, H., and Lakenby, J. Engineering behaviour of railway ballast – a critical review, Technical Report No. 1, RAIL-CRC Project No. 6, University of Wollongong, NSW, Australia. 2002.
- Indraratna, B., Ngo, N.T. and Rujikiatkamjorn, C. Behaviour of geogrid-reinforced ballast under various levels of fouling. *Geotextiles and Geomembranes*. 2011b. 29(3): p.313-322
- Indraratna, B., Tennakoon, N., Nimbalkar, S. and Rujikiatkamjorn, C. Behaviour of Clay Fouled Ballast under Drained Triaxial Testing. *Géotechnique*, 2013. 63(5): p.410-419.
- Meyerhof, G.G . Ultimate bearing capacity on footing on sand layer overlying clay. *Canadian Geotech. J.*, 1974. 11(2): p.223-229.

Meyerhof, G.G and Hanna, A. M. Ultimate bearing capacity of foundations on layered soils under inclined load. Canadian Geotech. J., 1978. 15(4): p.565-572

Pilgrim, D. H. Australian rainfall and runoff: a guide to flood estimation, Institution of Engineers, Australia, 1997: p.15-54.

Reddy A. S. and Srinivasan R. J. Bearing capacity of footings on layered clays," Journal of Soil Mechanics and Foundations Division. Proceedings of the American Society of Civil Engineers. 1967. 3(SM2): p.83-100.

Sattler, P., Fredlund, D.G., Klassen, M.J., Jubien, W.B., and Rowan W.G. Bearing capacity approach to Railway design, utilising subgrade metric suction. Transportation Research Board, Transportation Research Record 1241, 198: p.27-33.

Selig, E. T. and Waters, J. M. Track Geotechnology and Substructure management. Thomas Telford, U.K. 1994.

Suiker, A. S. J., Selig, E. T. & Frenkel, R. Static and cyclic Triaxial testing of Ballast and Subballast. J. of Geotech. Geoenviron. Engng ASCE. 2005. 131(6): p.771-782.

Tennakoon, N and Indraratna B. Behaviour of clay-fouled ballast under cyclic loading. Géotechnique, 2014. 64(6): p.502-506.

Tennakoon, N., Indraratna, B., Rujikiatkamjorn, C., Nimbalkar, S. and Neville, T. The role of ballast fouling characteristics on the drainage capacity of rail substructure. ASTM Geotechnical Testing Journal. 2012. 35(4): p.1-12.